A VARIATIONAL APPROACH TO MODELING SLOW PROCESSES IN STOCHASTIC DYNAMICAL SYSTEMS[*]

FRANK NOÉ[†] AND FELIKS NÜSKE[†]

Abstract. The slow processes of metastable stochastic dynamical systems are difficult to access by direct numerical simulation due to the sampling problems. Here, we suggest an approach for modeling the slow parts of Markov processes by approximating the dominant eigenfunctions and eigenvalues of the propagator. To this end, a variational principle is derived that is based on the maximization of a Rayleigh coefficient. It is shown that this Rayleigh coefficient can be estimated from statistical observables that can be obtained from short distributed simulations starting from different parts of state space. The approach forms a basis for the development of adaptive and efficient computational algorithms for simulating and analyzing metastable Markov processes while avoiding the sampling problem. Since any stochastic process with finite memory can be transformed into a Markov process, the approach is applicable to a wide range of processes relevant for modeling complex real-world phenomena.

1. Introduction. In this article, we consider continuous-time Markov processes $\mathbf{z}_t \in \Omega$ living in a usually large state space Ω that is either continuous or discrete. The process $\mathbf{z}_t$ is considered to be sufficiently ergodic such that a unique stationary density (invariant measure) μ exists. Independent of the details of the dynamics (such as system size, potential, stochastic coupling, etc.), there exists a family of linear propagators $\mathcal{P}(\tau)$ which evolve the probability density of states ρ_τ as

$$(1.1) \qquad \rho_\tau = \mathcal{P}(\tau)\,\rho_0.$$

Continuous-time Markov processes are useful models of real-world processes in a variety of areas [44]. Examples include macroscopic phenomena such as the evolution of financial and climate systems [24, 30], as well as microscopic dynamics such as the diffusion of cells in liquids [1], the diffusion of biomolecules within cells [41], the stochastic reaction dynamics of chemicals at surfaces [31], and the stochastic dynamics governing the structural dynamics of molecules [2]. Often, these dynamics are metastable; i.e., they consist of slow processes between sets of state space that have long lifetimes. In macromolecules, such slowly exchanging sets are called conformations, and hence the union of the slowest dynamical processes there are termed conformation dynamics [35, 37].

In practice, the slow dynamical processes are the ones which pose the greatest difficulties to direct numerical simulation as they require the longest simulation times. An extreme example is the atomistic simulation of solvated biomolecules which would require the propagation of a system with 10^4–10^6 particles for 10^7–10^{10} time-steps, a

[†]Department of Mathematics and Research Center MATHEON, FU Berlin, 14195 Berlin, Germany (frank.noe@fu-berlin.de, feliks.nueske@fu-berlin.de).

task that is intractable or hardly tractable even with special-purpose supercomputers [39]. However, the slowest processes are also the ones that are the most interesting in many systems. They often correspond to rare events that change the global structure and/or the functional behavior of the system. For example, in macromolecular systems, the slowest events often correspond to functional conformational changes such as folding, binding, or catalysis [28, 45, 7, 21]. Therefore, a method is sought that models the slow dynamical processes of continuous-time Markov processes accurately and ideally in a way that supports the efficient simulation of these processes without the need to solve the full direct numerical simulation problem.

Especially in statistical physics, many theories and methods have been proposed for modeling slow dynamical processes. Examples are rate theories that describe the passage rate of a process across a surface that separates metastable states [15, 20], pathway-based theories and methods that describe the transition dynamics of a system from a subset A to a subset B of state space [14, 3, 25], and network-based approaches that attempt to coarse-grain the high-dimensional dynamics to a network of discrete jump events between substates or landmarks [47, 48]. These approaches usually assume a separation of timescales between the slow and the fast processes that results from vanishing smallness parameters (e.g., noise intensity, temperature). In these cases, the mathematical analysis can be based on large deviation estimates and variational principles [16, 14].

In this article, we consider a more general approach to describing slow dynamical processes. When the operator $\mathcal{P}$ is compact and self-adjoint, (1.1) can be decomposed into the propagator's spectral components,

$$(1.2) \qquad \rho_\tau = \mu + \sum_{i=2}^{m} a_i(\rho_0)\lambda_i(\tau)l_i + \mathcal{P}_{\text{fast}}(\tau)\,\rho_0,$$

where $\mu, l_2, l_3, \ldots$ are the propagator's eigenfunctions and $\lambda_i(\tau) = \exp(-\kappa_i\tau)$ (sorted in nonascending order) are the propagator's real-valued eigenvalues that decay exponentially in time with rates κ_i. $a_i(\rho_0)$ are factors depending on the initial density ρ_0. Here we consider the situation that the eigenspaces of slow and fast processes are orthogonal. For example, in the important case that the system studied is a microscopic physical system in thermal equilibrium, such that the process $\mathbf{z}_t$ is reversible with respect to the invariant density μ, the eigenspaces of slow and fast processes are orthogonal for any choice of m. In such a case, m is a model parameter that can be chosen to distinguish the m slow processes of interest from the fast processes $\mathcal{P}_{\text{fast}}(\tau)$ that are not of interest. For initial densities $\rho_0 \in \text{span}\{\mu, l_2, \ldots, l_m\}$, the term for fast processes in (1.2) vanishes and the propagation can be performed exactly using only the dominant eigenfunctions. Note that (1.2) represents the formulation of the dynamical process problem as a multiscale problem in time: μ represents the timescale ∞, $t_2 = \kappa_2^{-1} = -\tau/\ln\lambda_2$ is the slowest dynamical process, etc. This formulation thus allows essential characteristics of the dynamical process to be described by treating its scales *separately*. The relation between dominant eigenvalues, exit times and rates, and metastable sets has been studied by asymptotic expansions in certain smallness parameters as well as by functional analytic means without any relation to smallness parameters [23, 12, 46, 4, 5]. In particular, [10, 11] established fundamental relations between the eigenvalues and eigenfunctions of $\mathcal{P}$ and metastable sets.

The task is now to approximate the propagator's dominant eigenfunctions $\mu, l_2, l_3, \ldots$ and eigenvalues λ_i. In other disciplines, variational principles have been worked out in order to approximate eigenfunctions and eigenvalues of known operators such

as a quantum-mechanical Hamiltonian [43]. In contrast, for many complex dynamical systems, $\mathcal{P}(\tau)$ is either not known explicitly or not available in a form that can be transformed into (1.2). Instead, $\mathcal{P}(\tau)$ is given implicitly through stochastic realizations of the process $\mathbf{z}_t$. Therefore, a variational principle is sought that allows eigenfunctions $\mu, l_2, l_3, \ldots$ and eigenvalues λ_i to be approximated through statistical observables of $\mathbf{z}_t$. Such a variational principle will be formulated in the present paper.

This problem has been studied extensively for specific functional forms of the eigenfunctions l_i. When l_i are approximated via characteristic functions on a given set decomposition of state space, i.e., $l_i \mu^{-1} \in \mathrm{span}\{\mathbf{1}_{S_1}, \ldots, \mathbf{1}_{S_n}\}$ with $S_j \subset \Omega$, the problem of finding the best approximation to eigenfunctions and eigenvalues is solved by a Markov model or Markov state model (MSM) [35, 4, 12, 34, 26, 22]. In another version of MSMs, l_i are approximated by committor functions between a few predefined "cores" that form a noncomplete subset of state space [8, 13, 36]. Basis functions that form a partition of unity are used in [49]. MSMs have been recently used a lot to model molecular dynamics processes, especially in conjunction with large amounts of distributedly simulated trajectories [42, 40, 9, 27, 8, 28]. Applications include conformational rearrangements and folding of peptides, proteins, and RNA [9, 29, 6, 28, 45, 26]. In this application area, MSMs have had significant impact because they can be estimated from relatively short simulation trajectories and yet allow the system behavior to be predicted at long timescales.

Despite this success, significant challenges remain. For example, in most current applications, the discretization of state space is done heuristically via a Voronoi partition of state space obtained from clustering available data points. The ability to construct a state space discretization adaptively would tremendously aid the construction of MSMs that are precise while avoiding the use of too many states. Such an adaptive discretization must be guided by an objective function that somehow measures the error made by the model. A bound to the MSM discretization error has been derived in [34]. However, this error is not suitable for designing a constructive discretization approach, as its evaluation requires knowledge of the exact eigenfunctions. The variational principle derived in this paper uses only statistical observables and is henceforth the basis for such a constructive approach to adaptive discretization. Furthermore, it is shown that existing Markov modeling approaches can be understood as a constrained optimal solution of the variational principle via a Ritz or Roothaan–Hall method with different choices of basis sets. Based upon this formulation, further development of basis sets appropriate for describing complex molecular conformation dynamics can be made.

The article is organized as follows: In section 2 a variational principle is formulated where the dominant eigenfunctions of stochastic dynamical systems are approximated by maximizing a Rayleigh coefficient, which—in the limit of the exact solution—is identical to the true eigenvalues. This Rayleigh coefficient is linked to the computation of correlation functions that can be evaluated without explicit knowledge of the propagator $\mathcal{P}$. Section 3 makes considerations concerning which types of functions may be practically useful to construct an approximation to (1.2) in complex systems. Section 4 shows numerical experiments on a diffusion process in a one-dimensional double-well potential. Section 5 concludes this study and makes suggestions for future research.

2. Variational principle for conformation dynamics.

2.1. Basics. Let Ω be a state space, and let us use $\mathbf{x}, \mathbf{y}$ to denote points in this state space. We consider a Markov process $\mathbf{z}_t$ on Ω which is stationary and ergodic

with respect to its unique stationary (invariant) distribution $\mu(\mathbf{x}) \equiv p(\mathbf{z}_t = \mathbf{x}) \, \forall t$. The dynamics of the process $\mathbf{z}_t$ are characterized by the transition density

$$(2.1) \qquad p(\mathbf{x}, \mathbf{y}; \tau) = p(\mathbf{z}_{t+\tau} = \mathbf{y} \mid \mathbf{z}_t = \mathbf{x}),$$

which we assume to be independent of the time t. The correlation density, i.e., the probability density of finding the process at points $\mathbf{x}$ and $\mathbf{y}$ at a time spacing of τ, is then defined by

$$(2.2) \qquad C(\mathbf{x}, \mathbf{y}; \tau) = \mu(\mathbf{x}) \, p(\mathbf{x}, \mathbf{y}; \tau) = p(\mathbf{z}_{t+\tau} = \mathbf{y}, \mathbf{z}_t = \mathbf{x}).$$

We further assume $\mathbf{z}_t$ to be reversible with respect to its stationary distribution, i.e.,

$$(2.3) \qquad \mu(\mathbf{x}) \, p(\mathbf{x}, \mathbf{y}; \tau) = \mu(\mathbf{y}) \, p(\mathbf{y}, \mathbf{x}; \tau),$$
$$(2.4) \qquad C(\mathbf{x}, \mathbf{y}; \tau) = C(\mathbf{y}, \mathbf{x}; \tau).$$

Reversibility is not strictly necessary but tremendously simplifies the forthcoming expressions and their interpretation [34]. In physical simulations, reversibility is the consequence of the simulation system being in thermal equilibrium with its environment; i.e., the dynamics in the system are purely a consequence of thermal fluctuations and there are no external driving forces.

If, at time $t = 0$, the process is distributed according to a probability distribution ρ_0, the corresponding distribution at time τ is given by

$$(2.5) \qquad \rho_\tau(\mathbf{y}) = \int_\Omega d\mathbf{x} \, \rho_0(\mathbf{x}) \, p(\mathbf{x}, \mathbf{y}; \tau) =: \mathcal{P}(\tau)\rho_0.$$

The time evolution of probability densities can be seen as the action of a linear operator $\mathcal{P}(\tau)$, called the propagator of the process. This is a well-defined operator on the Hilbert space $L^2_{\mu^{-1}}(\Omega)$ of functions which are square-integrable with respect to the weight function μ^{-1}. The scalar-product on this space is given by

$$(2.6) \qquad \langle u \mid v \rangle_{\mu^{-1}} = \int_\Omega d\mathbf{x} u(\mathbf{x}) v(\mathbf{x}) \mu^{-1}(\mathbf{x}).$$

If we assume the transition density to be a smooth and bounded function of $\mathbf{x}$ and $\mathbf{y}$, the propagator can be shown to be bounded, with operator norm less than or equal to one. Since the stationarity of μ implies $\mathcal{P}(\tau)\mu = \mu$, we even have $\|\mathcal{P}(\tau)\| = 1$. Reversibility allows us to show that the propagator is self-adjoint and compact. Furthermore, using the definition of the transition density, we can show that $\mathcal{P}(\tau)$ satisfies a Chapman–Kolmogorov equation: For times $\tau_1, \tau_2 \geq 0$, we have

$$(2.7) \qquad \mathcal{P}(\tau_1 + \tau_2) = \mathcal{P}(\tau_1)\mathcal{P}(\tau_2).$$

2.2. Spectral decomposition. It follows from the above arguments that $\mathcal{P}(\tau)$ possesses a sequence of real eigenvalues $\lambda_i(\tau)$, with $|\lambda_i(\tau)| \leq 1$ and $|\lambda_i(\tau)| \to 0$. Each of these eigenvalues corresponds to an eigenfunction $l_i \in L^2_{\mu^{-1}}(\Omega)$. The functions l_i form an orthonormal basis of the Hilbert space $L^2_{\mu^{-1}}(\Omega)$. Clearly, $\lambda_1(\tau) = 1$ is an eigenvalue with eigenfunction $l_1 = \mu$. In many applications, we can assume that $\lambda_1(\tau)$ is nondegenerate and -1 is not an eigenvalue. Additionally, there usually is a number m of positive eigenvalues

$$(2.8) \qquad 1 = \lambda_1(\tau) > \lambda_2(\tau) > \cdots > \lambda_m(\tau),$$

which are separated from the remaining spectrum. Due to the Chapman–Kolmogorov equation, each eigenvalue $\lambda_i(\tau)$ decays exponentially in time; i.e., we have

$$\lambda_i(\tau) = \exp(-\kappa_i \tau) \tag{2.9}$$

for some rate $\kappa_i \geq 0$. Clearly, $\kappa_1 = 0$, $\kappa_2, \ldots, \kappa_m$ are close to zero, and all remaining rates are significantly larger than zero. If we now expand a function $u \in L^2_{\mu^{-1}}(\Omega)$ in terms of the functions l_i, i.e.,

$$u = \sum_{i=1}^{\infty} \langle u \mid l_i \rangle_{\mu^{-1}} l_i, \tag{2.10}$$

we can decompose the action of the operator $\mathcal{P}(\tau)$ into its action on each of the basis functions:

$$
\begin{aligned}
\mathcal{P}(\tau)u &= \sum_{i=1}^{\infty} \langle u \mid l_i \rangle_{\mu^{-1}} \mathcal{P}(\tau)l_i \\
&= \sum_{i=1}^{\infty} \lambda_i(\tau) \langle u \mid l_i \rangle_{\mu^{-1}} l_i \\
&= \sum_{i=1}^{\infty} \exp(-\kappa_i \tau) \langle u \mid l_i \rangle_{\mu^{-1}} l_i.
\end{aligned}
\tag{2.11}
$$

For lag times $\tau \gg \frac{1}{\kappa_{m+1}}$, all except the first m terms in the above sum have become very small [34], and to a good approximation we have

$$\mathcal{P}(\tau)u \approx \sum_{i=1}^{m} \exp(-\kappa_i \tau) \langle u \mid l_i \rangle_{\mu^{-1}} l_i. \tag{2.12}$$

Knowledge of the dominant eigenfunctions and eigenvalues is therefore most helpful to the understanding of the process.

Remark 2.1. Instead of the propagator $\mathcal{P}(\tau)$, one can also consider the transfer operator $\mathcal{T}(\tau)$, defined for functions $u \in L^2_{\mu}(\Omega)$ by

$$\mathcal{T}(\tau)u(\mathbf{y}) = \frac{1}{\mu(\mathbf{y})} \int_{\Omega} d\mathbf{x} p(\mathbf{x}, \mathbf{y}; \tau)\mu(\mathbf{x})u(\mathbf{x}). \tag{2.13}$$

Using the unitary multiplication operator $\mathcal{M} : L^2_{\mu}(\Omega) \mapsto L^2_{\mu^{-1}}(\Omega)$, defined by

$$\mathcal{M}u(\mathbf{x}) = \mu(\mathbf{x})u(\mathbf{x}), \tag{2.14}$$

we have

$$\mathcal{P}(\tau) = \mathcal{M}\mathcal{T}(\tau)\mathcal{M}^{-1}, \tag{2.15}$$

and consequently the transfer operator inherits all of the above properties from $\mathcal{P}(\tau)$. In particular, there is a sequence of eigenfunctions

$$r_i = \mu^{-1}l_i \tag{2.16}$$

of $\mathcal{T}(\tau)$, corresponding to the same eigenvalues $\lambda_i(\tau)$, which are normalized with respect to the scalar-product weighted with μ instead of μ^{-1}. Especially, we have $r_1 = \mu^{-1}\mu = 1$. The two operators can be treated as equivalent, and all of the above could have been formulated in terms of $\mathcal{T}(\tau)$ as well.

2.3. Rayleigh variational principle. In nontrivial dynamical systems neither the correlation densities $p(\mathbf{x}, \mathbf{y}; \tau)$ and $C(\mathbf{x}, \mathbf{y}; \tau)$ nor the eigenvalues $\lambda_i(\tau)$ and eigenfunctions l_i are analytically available. This section provides a variational principle based on which these quantities can be estimated from simulation data generated by the dynamical process $\mathbf{z}_t$. For this, the formalism introduced above is used to formulate the Rayleigh variational principle used in quantum mechanics [43] for Markov processes.

Let f be a real-valued function of state, $f = f(\mathbf{x}) : \Omega \to \mathbb{R}$. Its autocorrelation with respect to the stochastic process $\mathbf{z}_t$ is given by

(2.17)
$$\mathrm{acf}(f; \tau) = \mathbb{E}[f(\mathbf{z}_0) \, f(\mathbf{z}_\tau)] = \int_{\mathbf{x}} \int_{\mathbf{y}} d\mathbf{x} \, d\mathbf{y} \, f(\mathbf{x}) \, C(\mathbf{x}, \mathbf{y}; \tau) \, f(\mathbf{y}) = \langle \mathcal{P}(\tau)\mu f \mid \mu f \rangle_{\mu^{-1}}.$$

In the Dirac notation often used in physical literature, integrals such as the one above may be abbreviated by $\mathbb{E}[f(\mathbf{x}_0) \, f(\mathbf{x}_\tau)] = \langle \mu f \mid \mathcal{P}(\tau) \mid \mu f \rangle$.

THEOREM 2.2. *The autocorrelation function of a weighted eigenfunction $r_k = \mu^{-1}l_k$ is its eigenvalue $\lambda_k(\tau)$:*

(2.18)
$$\mathrm{acf}(r_k; \tau) = \mathbb{E}\left[r_k(\mathbf{z}_0) \, r_k(\mathbf{z}_\tau)\right] = \lambda_k(\tau).$$

Proof. Using (2.17) with $f = \mu^{-1}l_k$, it directly follows that

(2.19)
$$\begin{aligned}
\mathrm{acf}(r_k; \tau) &= \langle \mathcal{P}(\tau)l_k \mid l_k \rangle_{\mu^{-1}} \\
&= \lambda_k(\tau) \langle l_k \mid l_k \rangle_{\mu^{-1}} \\
&= \lambda_k(\tau). \quad \square
\end{aligned}$$

THEOREM 2.3. *Let $\hat{l}_2$ be an approximate model for the second eigenfunction, which is normalized and orthogonal to the true first eigenfunction:*

(2.20)
$$\langle \hat{l}_2, \mu \rangle_{\mu^{-1}} = 0,$$

(2.21)
$$\langle \hat{l}_2, \hat{l}_2 \rangle_{\mu^{-1}} = 1.$$

Then we find for $\hat{r}_2 = \mu^{-1}\hat{l}_2$

(2.22)
$$\mathrm{acf}(\hat{r}_2; \tau) = \mathbb{E}\left[\hat{r}_2(\mathbf{z}_0) \, \hat{r}_2(\mathbf{z}_\tau)\right] \leq \lambda_2(\tau).$$

Proof. The proof is an application of the Rayleigh variational method to the operator $\mathcal{P}(\tau)$. If $\hat{l}_2$ is written in terms of the basis of eigenfunctions l_i,

(2.23)
$$\hat{l}_2 = \sum_{i=2}^{\infty} a_i l_i,$$

where $a_1 = 0$ because of the orthogonality condition, we find

(2.24)
$$\begin{aligned}
\mathrm{acf}(\hat{r}_2; \tau) &= \left\langle \mathcal{P}(\tau)\hat{l}_2 \mid \hat{l}_2 \right\rangle_{\mu^{-1}} \\
&= \sum_{i,j=2}^{\infty} a_i a_j \left\langle \mathcal{P}(\tau)l_i \mid l_j \right\rangle_{\mu^{-1}} \\
&= \sum_{i,j=2}^{\infty} a_i a_j \lambda_i(\tau) \left\langle l_i \mid l_j \right\rangle_{\mu^{-1}} \\
&= \sum_{i=2}^{\infty} a_i^2 \lambda_i(\tau) \\
&\leq \lambda_2(\tau) \sum_{i=2}^{\infty} a_i^2 \\
&= \lambda_2(\tau).
\end{aligned}$$

The estimate in the second-to-last row is due to the ordering of the eigenvalues, and the last equality results from the normalization condition (2.21) and Parseval's identity.   □

COROLLARY 2.4. *Similarly, let $\hat{l}_k$ be an approximate model for the kth eigenfunction, with the normalization and orthogonality constraints*

$$(2.25) \qquad \langle \hat{l}_k, l_i \rangle_{\mu^{-1}} = 0 \quad \forall i < k,$$
$$\langle \hat{l}_k, \hat{l}_k \rangle_{\mu^{-1}} = 1.$$

Then

$$(2.26) \qquad \mathrm{acf}(\hat{r}_k; \tau) = \mathbb{E}\left[\hat{r}_k(\mathbf{z}_0)\,\hat{r}_k(\mathbf{z}_\tau)\right] \le \lambda_k(\tau).$$

The proof is analogous to that of Theorem 2.3.

Remark 2.5. Estimates improving upon those of Theorems 2.2 and 2.3 and Corollary 2.4 have been obtained in [22] for characteristic functions. With a redefinition of the terminology, they can be directly transferred to the case of mutually orthonormal basis functions. It would be interesting to study the applicability of these results to more general cases. However, obtaining such estimates is not the focus of the present paper.

Remark 2.6. The variational principle given by Theorems 2.2 and 2.3 and Corollary 2.4 is fulfilled for $\hat{l}_k$ with $k > 2$ only if the $k - 1$ dominant eigenfunctions are already known.

In particular, the first eigenfunction, i.e., the stationary density, must be known. In practice, these eigenfunctions are approximated by solving a variational principle. Nonetheless, some basic statements can be made even if no eigenfunction is known exactly. For example, it is trivial that when the estimated stationary density $\hat{\mu}$ is used in Theorem 2.2, then the estimate of the first eigenvalue is still always correctly 1,

$$(2.27) \qquad \mathrm{acf}(\hat{\mu}^{-1}\hat{\mu}; \tau) = \mathrm{acf}(1; \tau) = 1,$$

and from Theorems 2.2 and 2.3 it follows that for any function $\hat{r}_k \ne \hat{\mu}$

$$(2.28) \qquad \mathrm{acf}(\hat{r}_k; \tau) < 1.$$

Hence the eigenvalue 1 is simple and dominant also when estimating eigenvalues from data.

Remark 2.7. An important insight at this point is that a variational principle of conformation dynamics can be formulated in terms of correlation functions. In contrast to quantum mechanics or other fields where the variational principle has been successfully employed, no closed-form expression of the operator $\mathcal{P}(\tau)$ is needed. The ability to express the variational principle in terms of correlation functions with respect to $\mathcal{P}(\tau)$ means that the eigenvalues to be maximized can be directly estimated from simulation data. If statistically sufficient realizations of $\mathbf{z}_t$ are available, then the autocorrelation function can be estimated via

$$(2.29) \qquad \mathrm{acf}(\hat{r}_k; \tau) = \mathbb{E}(\hat{r}_k(\mathbf{z}_0)\hat{r}_k(\mathbf{z}_\tau)) \approx \frac{1}{N} \sum \hat{r}_k(\mathbf{z}_0)\hat{r}_k(\mathbf{z}_\tau),$$

where N is the number of simulated time windows of length τ. We will try to use this in the application of the method.

2.4. Ritz method. The Ritz method is a systematic approach for finding the best possible approximation to the m first eigenfunctions of an operator simultaneously in terms of a linear combination of orthonormal functions [32]. Here the Ritz method is simply restated in terms of the present notation. Let $\chi_i : \Omega \to \mathbb{R}$, $i \in \{1, \dots, m\}$, be a set of m orthonormal basis functions,

$$(2.30) \qquad \langle \chi_i, \chi_j \rangle_{\mu^{-1}} = \delta_{ij},$$

and let $\boldsymbol{\chi}$ denote the vector of these functions,

$$(2.31) \qquad \boldsymbol{\chi}(\mathbf{x}) = [\chi_1(\mathbf{x}), \dots, \chi_m(\mathbf{x})]^T.$$

We seek a coefficient matrix $\mathbf{B} \in \mathbb{R}^{m \times m}$,

$$(2.32) \qquad \mathbf{B} = [\mathbf{b}_1, \dots, \mathbf{b}_m],$$

with the column vectors $\mathbf{b}_i = [b_{i1}, \dots, b_{im}]^T$ that approximate the eigenfunctions of the propagator as

$$(2.33) \qquad \hat{l}_i(\mathbf{x}) = \mathbf{b}_i^T \boldsymbol{\chi}(\mathbf{x}) = \sum_{j=1}^{m} b_{ij} \chi_j(\mathbf{x})$$

with respect to the constraint that the functions $\hat{l}_i$ are also normalized. It turns out that the solution $\mathbf{B}$ to the eigenvalue equation

$$(2.34) \qquad \mathbf{HB} = \mathbf{B}\hat{\boldsymbol{\Lambda}},$$

with individual eigenvalue/eigenvector pairs

$$(2.35) \qquad \mathbf{Hb}_i = \mathbf{b}_i \hat{\lambda}_i$$

and density matrix $\mathbf{H} = [h_{ij}]$ defined by

$$(2.36) \qquad h_{ij} = \int_{\mathbf{x}} \int_{\mathbf{y}} d\mathbf{x} \, d\mathbf{y} \mu^{-1}(\mathbf{x}) \, \chi_i(\mathbf{x}) \, C(\mathbf{x}, \mathbf{y}; \tau) \, \mu^{-1}(\mathbf{y}) \chi_j(\mathbf{y})$$

$$(2.37) \qquad = \mathbb{E}[\mu^{-1}\chi_i(\mathbf{z}_0) \, \mu^{-1}\chi_j(\mathbf{z}_\tau)],$$

yields the desired result. More precisely, the eigenvector $\mathbf{b}_1$ corresponding to the greatest eigenvalue $\hat{\lambda}_1$ from (2.35) contains the coefficients of the linear combination which maximizes the Rayleigh coefficient among the functions χ_i, and this maximum is given by $\hat{\lambda}_1$. Consequently, $\hat{\lambda}_1$ should be as close as possible to $\lambda_1 = 1$, and the function generated from $\mathbf{b}_1$ should model the stationary density l_1. But furthermore, the remaining eigenvalues and eigenvectors generated from (2.34) can be used as estimates of the other eigenvalues $\lambda_2, \dots, \lambda_m$.

COROLLARY 2.8. *The second estimated eigenvalue $\hat{\lambda}_2$ from (2.35) satisfies $\hat{\lambda}_2 \leq \lambda_2$.*

Proof. First of all, note that $\langle \hat{l}_2 \mid \hat{l}_1 \rangle_{\mu^{-1}} = 0$ by the orthogonality of the eigen-

vectors of the matrix $\mathbf{H}$. For the same reason, we find that

$$
\begin{aligned}
\left\langle \mathcal{P}(\tau)\hat{l}_1 \mid \hat{l}_2 \right\rangle_{\mu^{-1}} &= \sum_{i,j=1}^{m} b_{1i}b_{2j} \left\langle \mathcal{P}(\tau)\chi_i \mid \chi_j \right\rangle_{\mu^{-1}} \\
&= \sum_{i,j=1}^{m} b_{1i}b_{2j}h_{ij} \\
&= \hat{\lambda}_2 \sum_{i=1}^{m} b_{1i}b_{2i}
\end{aligned}
$$

(2.38)
$$
= 0.
$$

Now, let $\hat{l} = x\hat{l}_1 + y\hat{l}_2$ be a linear combination of the first two model eigenfunctions which is normalized such that

$$
\begin{aligned}
1 &= \left\langle \hat{l} \mid \hat{l} \right\rangle_{\mu^{-1}} \\
&= x^2 \left\langle \hat{l}_1 \mid \hat{l}_1 \right\rangle_{\mu^{-1}} + y^2 \left\langle \hat{l}_2 \mid \hat{l}_2 \right\rangle_{\mu^{-1}}
\end{aligned}
$$

(2.39)
$$
= x^2 + y^2.
$$

Using (2.38) and (2.39), computing the Rayleigh coefficient of $\hat{l}$ results in

$$
\begin{aligned}
\left\langle \mathcal{P}(\tau)\hat{l} \mid \hat{l} \right\rangle_{\mu^{-1}} &= x^2 \left\langle \mathcal{P}(\tau)\hat{l}_1 \mid \hat{l}_1 \right\rangle_{\mu^{-1}} + y^2 \left\langle \mathcal{P}(\tau)\hat{l}_2 \mid \hat{l}_2 \right\rangle_{\mu^{-1}} \\
&= x^2\hat{\lambda}_1 + y^2\hat{\lambda}_2
\end{aligned}
$$

(2.40)
$$
= \hat{\lambda}_1 - y^2(\hat{\lambda}_1 - \hat{\lambda}_2),
$$

which is bounded from below by $\hat{\lambda}_2$. Clearly, there is a normalized linear combination $\hat{l}$ of $\hat{l}_1$ and $\hat{l}_2$ which is orthogonal to l_1. By (2.40) and the variational principle, we conclude that

$$
\begin{aligned}
\hat{\lambda}_2 &\le \left\langle \mathcal{P}(\tau)\hat{l} \mid \hat{l} \right\rangle_{\mu^{-1}} \\
&\le \lambda_2. \quad \square
\end{aligned}
$$

Remark 2.9. Due to the equality between (2.36) and (2.37) the elements of the $\mathbf{H}$ matrix can be estimated as correlation functions of a simulation of the process $\mathbf{z}_t$, as mentioned above, provided that a sufficient approximation of μ is at hand.

2.5. Roothaan–Hall method. The Roothaan–Hall method is a generalization of the Ritz method used for solving the linear parameter optimization problem for the case when the basis set is not orthogonal [33, 19]. Let the matrix $\mathbf{S} \in \mathbb{R}^{m \times m}$ with elements

(2.41)
$$
S_{ij} = \langle \chi_i, \chi_j \rangle_{\mu^{-1}}
$$

be the matrix of overlap integrals with the normalization conditions $S_{ii} = 1$. Note that $\mathbf{S}$ has full rank if and only if all χ_i are pairwise linearly independent. The optimal solutions $\mathbf{b}_i$ in the sense of (2.32)–(2.33) are found by the eigenvectors of the generalized eigenvalue problem,

(2.42)
$$
\mathbf{HB} = \mathbf{SB}\hat{\mathbf{\Lambda}},
$$

with the individual eigenvalue/eigenvector pairs

$$(2.43) \qquad \mathbf{H}\mathbf{b}_i = \mathbf{S}\mathbf{b}_i\hat{\lambda}_i.$$

Remark 2.10. The Ritz and Roothaan–Hall methods are useful for eigenfunction models that are expressed in terms of linear combinations of basis functions. Nonlinear parameter models can also be handled with nonlinear optimization methods. In such nonlinear cases it needs to be tested whether there is a unique optimum or not.

2.6. Markov state model. As an example, let $\{S_1, \ldots, S_n\}$ be pairwise disjoint sets partitioning Ω, and let $\pi_i = \int_{S_i} d\mathbf{x}\mu(\mathbf{x})$ be the stationary probability of set $S_i \subset \Omega$. Consider the piecewise constant functions

$$(2.44) \qquad \chi_i = \frac{1}{\sqrt{\pi_i}}\mathbf{1}_{S_i}$$

where $\mathbf{1}_{S_i}$ is the characteristic function that is 1 for $\mathbf{x} \in S_i$ and 0 elsewhere. Since $S_i \cap S_j = \emptyset \ \forall i \neq j$ these functions form a basis set with $\langle \chi_i, \chi_j \rangle_\mu = \delta_{ij}$. Therefore, we can directly use them as a model for the transfer operator eigenfunctions r_k. Evaluation of the corresponding $\mathbf{H}$ matrix yields

$$
\begin{aligned}
(2.45) \qquad h_{ij} &= \frac{1}{\sqrt{\pi_i \pi_j}} \int_{\mathbf{x}} \int_{\mathbf{y}} d\mathbf{x}\, d\mathbf{y}\, \mathbf{1}_{S_i}\, C(\mathbf{x}, \mathbf{y}; \tau)\, \mathbf{1}_{S_i} \\
&= \frac{1}{\sqrt{\pi_i \pi_j}} \int_{S_i} \int_{S_j} d\mathbf{x}\, d\mathbf{y}\, C(\mathbf{x}, \mathbf{y}; \tau) \\
&= \frac{c_{ij}}{\sqrt{\pi_i \pi_j}} \\
&= T_{ij} \sqrt{\frac{\pi_i}{\pi_j}},
\end{aligned}
$$

where $c_{ij} = \mathbb{P}(\mathbf{z}_{t+\tau} \in S_j, \mathbf{z}_t \in S_i)$ is the joint probability of observing the process in sets S_i and S_j with a time lag of τ, while $T_{ij} = \mathbb{P}(\mathbf{z}_{t+\tau} \in S_j \mid \mathbf{z}_t \in S_i)$ is the corresponding transition probability. Thus, computing the optimal step-function approximation to the true eigenfunctions $r_i = \mu^{-1}l_i$ and eigenvalues $\lambda_i(\tau)$ via the Ritz method is the same as computing eigenvalues and eigenvectors of the Markov model transition matrix $\mathbf{T} = [T_{ij}]$ and scaling them appropriately. This conclusion can also be obtained from [34] via a different route.

3. Modeling. Section 2 provided a general variational principle for approximating the dominant eigenvalues and eigenfunctions of Markov processes. In order to apply this principle to complex systems, a useful level of modeling the eigenfunctions in terms of basis functions needs to be found, and appropriate classes of basis functions must be identified. This section attempts a first approach to this problem by making general considerations for what modeling schemes might be appropriate.

3.1. Half-weighted eigenfunctions. Is it beneficial to directly model the propagator eigenfunctions l_k, their weighted counterparts $r_k = \mu^{-1}l_k$, or rather yet another set of functions? We would like to use a model that has the following properties:
  1. As basis functions χ_i it is preferred to use local functions, i.e., either functions with compact support, or at least with the property $\lim_{|\mathbf{x}| \to \infty} \chi_i(\mathbf{x}) \to 0$. Such locality is useful for directing the computational effort to specific regions

of state space and may aid the adaptive refinement of the eigenfunction approximation by specifically adding basis functions that add local refinements. Since we also aim to model eigenfunctions as linear combinations of basis functions, we cannot use the r_k eigenfunctions that are not local.

2. We would like to be able to precompute as many expressions as possible analytically. When using appropriate basis functions χ_i and χ_j it may be possible to calculate analytic solutions of the integrals $\langle \chi_i, \chi_j \rangle$, although this feature is usually destroyed when weighting with the stationary density, as in $\langle \chi_i, \chi_j \rangle_{\mu^{-1}}$. Therefore we will also avoid using the eigenfunctions l_k that would require such a weighting.

Consider a rewrite of (2.17) as follows:

$$\mathrm{acf}(r_k; \tau) = \int_{\mathbf{x}} \int_{\mathbf{y}} d\mathbf{x}\, d\mathbf{y}\, \mu^{-\frac{1}{2}}(\mathbf{x})\, l_k(\mathbf{x})\, \mu^{-\frac{1}{2}}(\mathbf{x})\, C(\mathbf{x}, \mathbf{y}; \tau)\, \mu^{-\frac{1}{2}}(\mathbf{y})\, \mu^{-\frac{1}{2}}(\mathbf{y})\, l_k(\mathbf{y})$$

$$(3.1) \qquad = \int_{\mathbf{x}} \int_{\mathbf{y}} d\mathbf{x}\, d\mathbf{y}\, \phi_k(\mathbf{x})\, S(\mathbf{x}, \mathbf{y}; \tau)\, \phi_k(\mathbf{y}),$$

where the "half-weighted" eigenfunctions

$$(3.2) \qquad \phi_i(\mathbf{x}) = \frac{l_i(\mathbf{x})}{\mu^{\frac{1}{2}}(\mathbf{x})}$$

and the "half-weighted" correlation density

$$(3.3) \qquad S(\mathbf{x}, \mathbf{y}; \tau) = \frac{C(\mathbf{x}, \mathbf{y}; \tau)}{\mu^{\frac{1}{2}}(\mathbf{x}) \mu^{\frac{1}{2}}(\mathbf{y})}$$

have been defined. Now, when modeling the half-weighted eigenfunctions ϕ_i using some basis set, the following nice properties are obtained:

1. Local basis functions can be used. This follows from $\lim_{|\mathbf{x}| \to \infty} \phi_i(\mathbf{x}) = \lim_{|\mathbf{x}| \to \infty} \mu^{\frac{1}{2}}(\mathbf{x}) r_i(\mathbf{x}) \to 0$.

2. The normalization condition requires a nonweighted scalar product:

$$(3.4) \qquad \langle l_i, l_j \rangle_{\mu^{-1}} = \left\langle \frac{l_i}{\mu^{1/2}}, \frac{l_j}{\mu^{1/2}} \right\rangle$$
$$= \langle \phi_i, \phi_j \rangle = \delta_{ij}.$$

3. When $\langle \chi_i, \chi_j \rangle$ is analytically computable and $\phi_k = \sum_i c_i \chi_i$, then $\langle \phi_k, \phi_k \rangle$ is also analytically computable.

4. The first half-weighted eigenfunction has eigenvalue 1 and is identical to the half-weighted stationary density

$$(3.5) \qquad \phi_1(\mathbf{x}) = \frac{l_1(\mathbf{x})}{\mu(\mathbf{x})^{1/2}} = \mu(\mathbf{x})^{1/2}.$$

5. When models of $\mu(\mathbf{x})^{1/2}$ and ϕ_k are available, the Rayleigh coefficient in (3.1) can be estimated numerically as the autocorrelation of $\frac{\phi_i}{\mu^{1/2}}$.

6. When defining a propagator $\mathcal{P}^*$ in half-weighted space via

$$(3.6) \qquad p_\tau(\mathbf{y}) = \mathcal{P}(\tau) \circ p_0(\mathbf{x}),$$

$$p_\tau(\mathbf{y}) = \int_{\mathbf{x}} d\mathbf{x}\, p(\mathbf{x})\, p(\mathbf{x}, \mathbf{y}; \tau),$$

$$\frac{p_\tau(\mathbf{y})}{\mu(\mathbf{y})^{1/2}} = \int_{\mathbf{x}} d\mathbf{x}\, \frac{p(\mathbf{x})}{\mu(\mathbf{x})^{1/2}} \frac{\mu(\mathbf{x})^{1/2}}{\mu(\mathbf{y})^{1/2}}\, p(\mathbf{x}, \mathbf{y}; \tau),$$

$$p_\tau^*(\mathbf{y}) = \int_{\mathbf{x}} d\mathbf{x}\, p_0^*(\mathbf{x})\, p^*(\mathbf{x}, \mathbf{y}; \tau),$$

$$= \mathcal{P}^*(\tau) \circ p_0^*(\mathbf{x}),$$

then $\mathcal{P}^*$ is self-adjoint and has orthogonal eigenfunctions

$$(3.7) \qquad \phi_i \lambda_i = \mathcal{P}^*(\tau) \phi_i.$$

It follows from Theorem 2.2 that the exact eigenvalues are calculated by the Rayleigh coefficients of the exact eigenfunctions,

$$(3.8) \qquad \lambda_i = \left\langle \mu^{-\frac{1}{2}} \phi_i \mid \mathcal{C} \mid \mu^{-\frac{1}{2}} \phi_i \right\rangle = \mathrm{acf}(\mu^{-\frac{1}{2}} \phi_i; \tau),$$

while they are approximated from below by the Rayleigh coefficients of the approximate eigenfunctions,

$$(3.9) \qquad \lambda_i \geq \hat{\lambda}_i = \left\langle \mu^{-\frac{1}{2}} \hat{\phi}_i \mid \mathcal{C} \mid \mu^{-\frac{1}{2}} \hat{\phi}_i \right\rangle = \mathrm{acf}(\mu^{-\frac{1}{2}} \hat{\phi}_i; \tau).$$

This Rayleigh coefficient can be directly sampled: for a given trajectory $\mathbf{z}_t$, it can be estimated as

$$(3.10) \qquad \lambda_i \geq \hat{\lambda}_i = \mathbb{E}_t \left[\hat{\mu}(\mathbf{z}_t)^{-\frac{1}{2}} \hat{\phi}_i(\mathbf{z}_t) \hat{\mu}(\mathbf{z}_{t+\tau})^{-\frac{1}{2}} \hat{\phi}_i(\mathbf{z}_{t+\tau}) \right].$$

Thus, for a given trajectory $\mathbf{z}_t$, the optimal eigenfunctions $\hat{\phi}_i$ can be calculated by maximizing the Rayleigh coefficient, using, e.g., the Ritz or the Roothaan–Hall method.

3.2. Gaussian basis functions. In complex dynamical processes, such as molecular dynamics of biomolecules, one has to devise basis sets that can be evaluated in high dimensions. While the present work provides merely a starting point for identifying appropriate basis sets that go beyond common choices such as the step function basis or the committor basis, we here suggest a possible choice that is potentially applicable to the molecular dynamics setting. Empirically, it has been found that the stationary densities of biomolecules in the essential subspace are often clustered [18]. Therefore, we put forward the idea that $\mu(\mathbf{x})^{1/2}$ and the other half-weighted eigenfunctions can be approximated by a Gaussian mixture.

Let us thus assume that the state space Ω is a metric space with distance $d(\mathbf{x}, \mathbf{y})$, and let us model the half-weighted invariant density $\hat{\mu}(\mathbf{x})^{1/2}$ in terms of Gaussian basis functions:

$$(3.11) \qquad \hat{\mu}(\mathbf{x})^{1/2} = \sum_i a_i \exp\left(-\frac{d(\mathbf{x}, \mathbf{y}_i)}{2\sigma^2} \right),$$

where $a_i \in \mathbb{R}$, $\mathbf{y}_i \in \Omega$, and $\sigma \in \mathbb{R}$ are amplitude, mean, and shape parameters. The invariant density can then be analytically given:

$$\hat{\mu}(x) = \left(\hat{\mu}(x)^{1/2} \right)^2 = \left(\sum_i a_i \exp \left(-\frac{d(\mathbf{x}, \mathbf{y}_i)}{2\sigma^2} \right) \right)^2$$

$$(3.12) \qquad = \sum_i a_i^2 \exp \left(-\frac{d(\mathbf{x}, \mathbf{y}_i)}{\sigma^2} \right) + \sum_{i<j} 2 a_i a_j \exp \left(-\frac{d(\mathbf{x}, \mathbf{y}_i) + d(\mathbf{x}, \mathbf{y}_j)}{2\sigma^2} \right).$$

Furthermore, consider that the half-weighted eigenfunctions can be given in terms of the same Gaussian basis:

$$(3.13) \qquad \hat{\phi}_k(\mathbf{x}) = \sum_i b_{ki} \exp \left(-\frac{d(\mathbf{x}, \mathbf{y}_i)}{2\sigma^2} \right),$$

where b_{ki} must be appropriately chosen to guarantee orthogonality with respect to the invariant density. The corresponding unweighted eigenfunctions $\hat{r}_k$ are

$$(3.14) \qquad \hat{r}_k(x) = \frac{\hat{\phi}_k(x)}{\hat{\phi}_1(x)} = \frac{\sum_i b_{ki} \exp \left(-\frac{d(\mathbf{x}, \mathbf{y}_i)}{2\sigma^2} \right)}{\sum_i a_i \exp \left(-\frac{d(\mathbf{x}, \mathbf{y}_i)}{2\sigma^2} \right)},$$

which does not have a simple form, but can be evaluated pointwise. In order to enforce the normalization $\langle \hat{\phi}_k, \hat{\phi}_l \rangle = \delta_{kl}$ we consider

$$(3.15) \qquad \langle \hat{\phi}_k, \hat{\phi}_l \rangle = \int d\mathbf{x} \sum_i \sum_j b_{ki} b_{lj} \exp \left(-\frac{d(\mathbf{x}, \mathbf{y}_i) + d(\mathbf{x}, \mathbf{y}_j)}{2\sigma^2} \right),$$

which can be analytically evaluated when Ω is a Euclidean space.

Using Gaussian ansatz functions in half-weighted space may thus have important practical benefits. However, other basis sets, especially sets of radial basis functions other than Gaussians, may also be a good choice for high-dimensional systems that deserves further investigation.

4. Numerical examples.

4.1. Metastable potential from a Gaussian stationary density. The example is chosen such that it is tractable by direct grid discretization so as to be able to generate a reference solution. Different optimization methods for the variational problem and choices of basis sets are considered and illustrated. See Figure 4.1 for an illustration of the potential and its eigenvectors.

Let $\Omega = \mathbb{R}$ be our state space with points $x \in \Omega$. First, a "Gaussian hat" function is defined via

$$(4.1) \qquad gh(x; a, s) := \exp \left(-\frac{(x-a)^2}{2s^2} \right),$$

where $a \in \mathbb{R}$ is the mean and $s \in \mathbb{R}$ the standard deviation. We define a stationary density from two Gaussians:

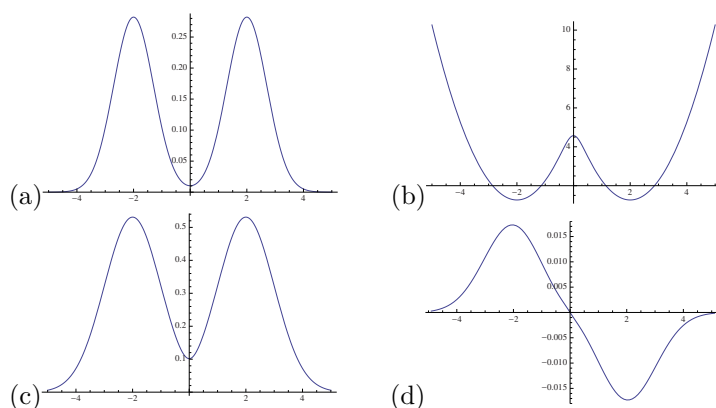$$\mu(x) := \frac{1}{2\sqrt{\pi}} \left(gh(x, -2, 1) + gh(x, 2, 1) \right).$$

Fig. 4.1. *Two-well potential with Smoluchowski dynamics, $\tau = 0.025$. (a) Double-Gaussian density $\mu(x)$, (b) the corresponding potential $U(x)$, (c) the half-weighted density $\phi_1(x) = \sqrt{\mu(x)}$, (d) slowest-process eigenfunction $\phi_2(x)$ from direct numerical solution.*

The corresponding dimensionless generating potential is given by

$$(4.2) \qquad U(x) = -\ln(\mu(x)),$$

which exerts a force on a particle at position x of

$$(4.3) \qquad f(x) = -\nabla U(x) = \frac{1}{\mu(x)}\frac{d}{dx}\mu(x).$$

Using Smoluchowski dynamics and Euler discretization, a time-step $x \xrightarrow{\tau} y$ is given by

$$(4.4) \qquad y = x + \tau f(x) + \sqrt{2\tau}\eta,$$

where η is a normally distributed random variable (white noise). The transition density can hence be written as

$$(4.5) \qquad p(x, y; \tau) = \mathcal{N}_y(x + \tau f(x), \sqrt{2\tau})$$

and the correlation density is given by

$$(4.6) \qquad C(x, y; \tau) = \mu(x)\, p(x, y; \tau).$$

Now we are concerned about estimation of eigenfunctions. The first half-weighted eigenfunction is the square root of the stationary density,

$$(4.7) \qquad \phi_1 = \sqrt{\mu(x)},$$

such that $\phi_1^2(x) = \mu(x)$. We here assume $\mu(x)$ to be known, although in practice it must be estimated.

4.2. Ritz method with characteristic functions (Markov state model). We aim to approximate the eigenvalues and eigenfunctions of the true propagator via the Ritz method described in section 2.4. Here, a basis set $\boldsymbol{\chi} = (\chi_1(x), \dots, \chi_N(x))^T$ consisting of $N = 20$ characteristic functions in the range $x \in [-6, 6]$ is defined by

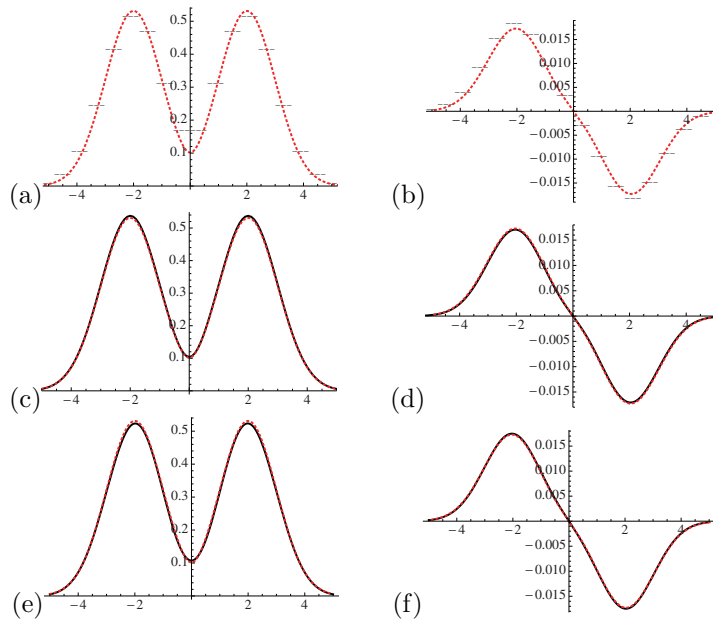$$(4.8) \qquad \chi_i = \frac{1}{\sqrt{\pi_i}}\mathbf{1}_{[-6+0.6i,\ -5.4+0.6i]},$$

FIG. 4.2. *Approximation to the eigenfunction shown in Figure* 4.1 *using different methods and basis sets. The true eigenvalues are* 1.0, 0.998913. *The reference solutions are shown as dotted lines, while the approximations are shown as solid lines.* (a), (b) *MSM/Ritz method with* 20 *characteristic functions in the range* $x \in [-6, 6]$. *Eigenvalues* 1.0, 0.980384. (c), (d) *Ritz method with a basis set of* 20 *Hermite functions. Eigenvalues* 1.0, 0.998913. (e), (f) *Roothaan–Hall method with a basis set of* 11 *Gaussians. Eigenvalues* 1.0, 0.995507.

where $\mathbf{1}_{[a,b]}$ is the characteristic function that is 1 on the interval $[a, b]$ and 0 outside, and $\pi_i = \int_{s_i} \mu(x)dx$ is the stationary probability of the set $S_i = [-6+0.6i, -5.4+0.6i]$. The corresponding density-matrix $\mathbf{H} = [h_{ij}] \in \mathbb{R}^{N \times N}$ defined by (Dirac notation)

$$(4.9) \qquad h_{ij} = \langle \chi_i \,|\, \mathcal{C} \,|\, \chi_j \rangle$$

takes the form

$$(4.10) \qquad h_{ij} = \frac{\sqrt{\pi_i} \int_{S_i} dx \, \int_{S_j} dy \, C(x, y; \, \tau)}{\sqrt{\pi_j}}$$

as in section 2.6.

The $\mathbf{H}$ matrix was calculated by direct numerical integration using *Mathematica* and the eigenvalue problem was subsequently solved, yielding the optimal coefficient vectors $\mathbf{c}_1$ and $\mathbf{c}_2$ that provide the approximations $\hat{\phi}_1 \approx \phi_1$, $\hat{\phi}_2 \approx \phi_2$ and $\hat{\lambda}_1 \approx \lambda_2$, $\hat{\lambda}_2 \approx \lambda_2$. The results are given in Figures 4.2(a) and (b), indicating that the eigenvalues are approximated to two significant digits, while the eigenfunctions retain a significant discretization error that arises from the step-function basis used.

4.3. Ritz method with a Hermite basis. In order to arrive at a smooth solution we employ the Ritz method with a smooth orthogonal function basis. Here, we choose the Hermite functions, defined by

$$(4.11) \qquad \psi_i(x) = (-1)^i (2^i i! \sqrt{\pi})^{-1/2} \mathrm{e}^{x^2/2} \frac{d^i}{dx^i} \mathrm{e}^{-x^2}.$$

The Hermite functions are local ($\lim_{|\mathbf{x}|\to\infty} \chi_i(\mathbf{x}) \to 0$) and are thus useful in modeling the behavior of the eigenfunctions ϕ_k where the stationary density is significantly larger than zero. The basis functions are defined to be the normalized Hermite functions with

$$\chi_i = \frac{\psi_i}{\sqrt{\langle \psi_i, \psi_i \rangle}} \tag{4.12}$$

such that $\langle \chi_i, \chi_j \rangle = \delta_{ij}$.

Using the basis set $\boldsymbol{\chi} = [\chi_0, \ldots, \chi_{19}]^T$, the $\mathbf{H}$ matrix was calculated by direct numerical integration using *Mathematica* and the Ritz method was used to approximate eigenvalues and eigenfunctions of the propagator. As shown in Figures 4.2(c) and (d), a nearly perfect approximation of both eigenvalues and eigenfunctions is obtained even though the number of basis functions used is identical to the MSM approach of the previous section. However, the MSM approach has the advantage that it can be employed in high-dimensional spaces, which is not the case with Hermite basis functions.

4.4. Roothaan–Hall method with a Gaussian basis. In order to attempt solving high-dimensional problems, one must resort to simple basis functions, ideally ones with analytical properties that can be practically evaluated in high-dimensional spaces. Therefore, we here suggest the use of Gaussian basis functions as described in section 3.2. In the one-dimensional case, the Gaussians used are

$$gh_i(x) = \exp\left(-\frac{(x-y_i)^2}{2\sigma^2}\right). \tag{4.13}$$

Here, we use $\sigma = 1$ and $y_i = (-5, -4, \ldots, 4, 5)$. Gaussian basis functions are not orthogonal. We therefore calculate the overlap matrix $\mathbf{S} = [s_{ij}]$ with

$$\begin{aligned} s_{ij} &= \langle gh_i, gh_j \rangle \\ &= \int_{-\infty}^{\infty} dx \, \exp\left(-\frac{(x-y_i)^2 + (x-y_j)^2}{2\sigma^2}\right) \end{aligned} \tag{4.14}$$

that can be evaluated analytically. The $\mathbf{H} = [h_{ab}]$ matrix is again defined by (Dirac notation)

$$h_{ab} = \langle gh_a \mid \mathcal{C} \mid gh_b \rangle. \tag{4.15}$$

Using the Roothaan–Hall method (section 2.5), the best approximation to the propagator eigenfunctions $\hat{\phi}_i = \langle \mathbf{b}_i, \boldsymbol{\chi} \rangle$ are found by the eigenvectors of the generalized eigenvalue problem

$$\mathbf{S}^{-1}\mathbf{H}\mathbf{b}_i = \hat{\lambda}_i \mathbf{b}_i. \tag{4.16}$$

As shown in Figures 4.2(c) and (d), an also nearly perfect approximation of both eigenvalues and eigenfunctions is achieved even though the basis is smaller than the previous basis sets. Since the Gaussian basis set is a good candidate for being used in high-dimensional spaces, this is probably the most useful result so far. Note that the matrix inversion $\mathbf{S}^{-1}$ can be efficiently calculated with sparse matrix methods when a cutoff is used to set nearly nonoverlapping pairs with $h_{ab} \approx 0$ to 0.
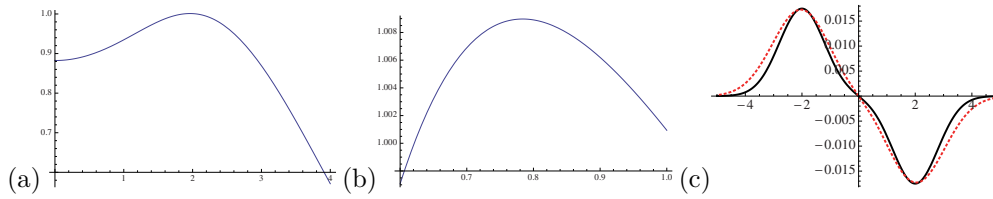
FIG. 4.3. *Nonlinear optimization of the propagator eigenfunctions.* (a) *Value of $\hat{\lambda}_2$ depending on y_2 and with fixed $s_2 = 0.8$.* (b) *Value of $\hat{\lambda}_2$ depending on s_2 with fixed $y_2 = 1$.* (c) *Approximation to ϕ_2 with $y_2 = 1$, $s_2 = 0.8$ (solid line), and reference solution for ϕ_2 (dotted line).*

4.5. Nonlinear optimization. The previous methods used exclusively linear combinations of basis functions. A greater degree of freedom in approximating the propagator eigenfunctions is achieved by using additional shape parameters in the basis functions. This, however, leads to a nonlinear optimization problem that is in general difficult to solve and may have multiple optima. However, we briefly illustrate the approach on our one-dimensional example. We make the ansatz for the second half-weighted eigenfunction:

$$(4.17) \qquad \hat{\phi}_2(x) = \frac{1}{Z} \left(-gh(x, y_2, s_2) + gh(x, y_2, s_2) \right),$$

$$Z = \left[\int_{-\infty}^{\infty} dx \left[-gh(x, y_2, s_2) + gh(x, y_2, s_2) \right] \right]^{1/2}.$$

The normalization constant makes sure that $\langle \hat{\phi}_2, \hat{\phi}_2 \rangle = 1$. The constraint $\langle \hat{\phi}_2, \phi_1 \rangle = 0$ is here ensured by the fact that ϕ_1 is an even function and $\hat{\phi}_2$ is an odd function.

The optimal parameters $\hat{y}_2$ and $\hat{s}_2$ are found by maximizing the Rayleigh coefficient:

$$(4.18) \qquad (\hat{y}_2, \hat{s}_2) = \arg\max_{y_2, s_2} \left\langle \frac{\hat{\phi}_2(y_2, s_2)}{\mu^{1/2}} \mid \mathcal{C} \mid \frac{\hat{\phi}_2(y_2, s_2)}{\mu^{1/2}} \right\rangle.$$

Figure 4.3 shows the results of varying y_2 and s_2 as well as the local optimum for $y_2 = 1$ and $s_2 = 0.8$. In this case, a good approximation to the eigenvector could be achieved with a 2-term ansatz function. However, the general usefulness of the nonlinear approach for high-dimensional problems remains to be evaluated.

4.6. Quartic potential. As a second numerical example, we use the diffusion in a one-dimensional quartic potential,

$$(4.19) \qquad V(x) = 3x^4 - 6x^2 + 3,$$

which has two minimum positions at $x = \pm 1$. We seek to estimate the second dominant eigenvalue $\lambda_2(\tau)$ and the corresponding timescale $t_2 = -\frac{\tau}{\log \lambda_2(\tau)}$ by applying the Roothaan–Hall method above with Gaussian functions. We will then compare the results to those obtained from an MSM discretization. First, we generate a sample trajectory of the process as in (4.4). Here, we used a time-step $\tau = 10^{-3}$ and a total number of steps $N = 10^7$. From this sample, we computed an estimate $\hat{\mu}$ of the stationary density. We then computed the MSM transition matrix and its eigenvalues, using a discretization of the state space into 100 sets.
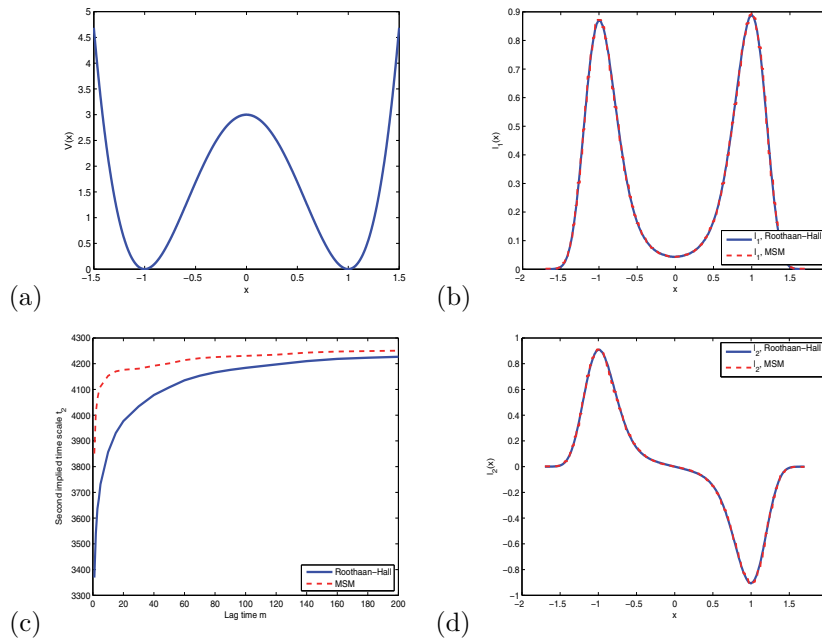
FIG. 4.4. *Application of the Roothaan–Hall method with Gaussian basis functions to a one-dimensional diffusion process, compared to a* 100-*set MSM discretization computed with the EMMA package* [38]. *(a) The potential function* V. *(b) Estimated stationary density* $\hat{l}_1$. *(c) Comparison of the second largest implied timescale* $t_2(\tau)$, *plotted against the lag time given in integer multiples* m *of the simulation step* τ. *(d) The second eigenfunction* $\hat{l}_2$ *as estimated from both methods.*

For the application of the Roothaan–Hall method, we picked thirteen Gaussian functions $\hat{\phi}_i$ with centers at

$$(4.20) \qquad x = -2, -1.5, -1.2, -1, -0.8, -0.5, 0, 0.5, 0.8, 1, 1.2, 1.5, 2.$$

The variances were set to 1 for the functions centered at $x = -2, -1.5, 0, 1.5, 2$, and to 0.5 for all others. Those functions were used as half-weighted basis functions, meaning that we computed the entries of the **H**-matrix according to

$$(4.21) \qquad h_{ij} = \frac{1}{N-m} \sum_{k=1}^{N-m} \hat{\mu}^{-1/2}(x_k)\hat{\phi}_i(x_k)\hat{\mu}^{-1/2}(x_{k+m})\hat{\phi}_j(x_{k+m}),$$

where m is an integer corresponding to the lag time $m\tau$. We similarly estimated the **S**-matrix and then solved the generalized eigenvalue problem (2.42).

The results displayed in Figure 4.4 show that we not only get a good approximation of both the first and second eigenfunction in terms of smooth functions, but most importantly the second largest eigenvalue $\lambda_2(\tau)$ and the corresponding time scale t_2 can be estimated comparably well with both methods. While 100 sets were used for the MSM discretization, only thirteen basis function were used for the Roothaan–Hall method.

5. Conclusions and outlook. Here, we have formulated a variational principle for Markov processes where the dominant eigenfunctions are approximated by maximizing a Rayleigh coefficient, which—in the limit of the exact eigenfunctions—is

identical to the true eigenvalues. This is the formulation needed to attack the problem of estimating the slow processes in stochastic dynamical systems with a much wider methodology than by the presently used class of Markov state models (MSMs). In particular, the entire toolbox of quantum mechanics, in which many decades of research have gone into the development of eigenfunction approximation methods for high-dimensional systems, becomes available.

From a practical point of view, the main achievement of the present study is that the Rayleigh coefficient can be estimated from simulation data, as it is equivalent to an autocorrelation function of the appropriately weighted test function. The autocorrelation estimates are such that they can be fed by many short simulations distributed across state space and do not require the direct simulation of the slow processes in a single long trajectory. This is an important advantage in dealing with the sampling problem that arises in simulating metastable dynamical systems.

One major use of the present approach will be to facilitate the development of adaptive discretization algorithms of high-dimensional state spaces for the computational characterization of complex dynamical processes. The Rayleigh coefficient derived here represents a practically accessible and theoretically solid functional to guide such an adaptive discretization algorithm. In contrast to MSMs, such an approximation approach does not necessarily need to use the same basis set for all eigenfunctions. Especially for reversible dynamics, different eigenfunctions can be approximated separately, thus possibly permitting the use of relatively small basis sets.

For a given class of dynamical systems, a basis set must be selected that is appropriate for modeling the regularity of the solution. For high-dimensional processes such as molecular dynamics, Gaussian basis functions might be a workable solution since they can be well combined with clustering-based identification of center positions and permit the analytical calculation of some quantities such as the overlap integral. An interesting alternative approach is to build the basis set upon weakly coupled subsets of internal molecular coordinates, as suggested in the mean field approach developed in [17]. The usefulness of these and other approaches for complex molecular systems will be investigated in future studies. Furthermore, subsequent studies will deal with the error caused by the projection on a finite-dimensional subspace depending on the choice of basis functions, as well as with statistical considerations, such as the efficient evaluation of uncertainties of the estimated Rayleigh coefficients.

REFERENCES

[1] K. ANGUIGE AND C. SCHMEISER, *A one-dimensional model of cell diffusion and aggregation, incorporating volume filling and cell-to-cell adhesion*, J. Math. Biol., 58 (2009), pp. 395–427.

[2] R. B. BEST AND G. HUMMER, *Coordinate-dependent diffusion in protein folding*, Proc. Natl. Acad. Sci. USA, 107 (2010), pp. 1088–1093.

[3] P. G. BOLHUIS, D. CHANDLER, C. DELLAGO, AND P. L. GEISSLER, *Transition path sampling: Throwing ropes over rough mountain passes, in the dark*, Annu. Rev. Phys. Chem., 53 (2002), pp. 291–318.

[4] A. BOVIER, M. ECKHOFF, V. GAYRARD, AND M. KLEIN, *Metastability in reversible diffusion processes.* I. *Sharp asymptotics for capacities and exit times*, J. Eur. Math. Soc. (JEMS),

6 (2004), pp. 399–424.

[5] A. BOVIER, M. ECKHOFF, V. GAYRARD, AND M. KLEIN, *Metastability in reversible diffusion processes*. II. *Precise asymptotics for small eigenvalues*, J. Eur. Math. Soc. (JEMS), 7 (2005), pp. 69–99.

[6] G. R. BOWMAN, K. A. BEAUCHAMP, G. BOXER, AND V. S. PANDE, *Progress and challenges in the automated construction of Markov state models for full protein systems*, J. Chem. Phys., 131 (2009), 124101.

[7] G. R. BOWMAN, V. A. VOELZ, AND V. S. PANDE, *Atomistic folding simulations of the five-helix bundle protein lambda* 6-85, J. Amer. Chem. Soc., 133 (2011), pp. 664–667.

[8] N. V. BUCHETE AND G. HUMMER, *Coarse master equations for peptide folding dynamics*, J. Phys. Chem. B, 112 (2008), pp. 6057–6069.

[9] J. D. CHODERA, K. A. DILL, N. SINGHAL, V. S. PANDE, W. C. SWOPE, AND J. W. PITERA, *Automatic discovery of metastable states for the construction of Markov models of macromolecular conformational dynamics*, J. Chem. Phys., 126 (2007), 155101.

[10] E. B. DAVIES, *Metastable states of symmetric Markov semigroups* I, Proc. London Math. Soc., 45 (1982), pp. 133–150.

[11] E. B. DAVIES, *Metastable states of symmetric Markov semigroups* II, J. London Math. Soc., 26 (1982), pp. 541–556.

[12] P. DEULFHARD, W. HUISINGA, A. FISCHER, AND C. SCHÜTTE, *Identification of almost invariant aggregates in reversibly nearly uncoupled Markov chains*, Linear Algebra Appl., 315 (2000), pp. 39–59.

[13] N. DJURDJEVAC, M. SARICH, AND C. SCHÜTTE, *Estimating the eigenvalue error of Markov state models*, Multiscale Model. Simul., 10 (2012), pp. 61–81.

[14] W. E AND E. VANDEN EIJNDEN, *Metastability, conformation dynamics, and transition pathways in complex systems*, in Multiscale Modelling and Simulation, Springer, Berlin, 2004, pp. 38–65.

[15] H. EYRING, *The activated complex in chemical reactions*, J. Chem. Phys., 3 (1935), pp. 107–115.

[16] M. FREIDLIN AND A. D. WENTZELL, *Random Perturbations of Dynamical Systems*, Springer, New York, 1998.

[17] G. FRIESECKE, O. JUNGE, AND P. KOLTAI, *Mean field approximation in conformation dynamics*, Multiscale Model. Simul., 8 (2009), pp. 254–268.

[18] H. GRUBMÜLLER, *Predicting slow structural transitions in macromolecular systems: Conformational flooding*, Phys. Rev. E, 52 (1995), pp. 2893–2906.

[19] G. G. HALL, *The molecular orbital theory of chemical valency*. VIII. *A method of calculating ionization potentials*, Proc. Roy. Soc. Lond. Ser. A, 205 (1951), pp. 541–552.

[20] P. HÄNGGI, P. TALKNER, AND M. BORKOVEC, *Reaction rate theory: Fifty years after Kramers*, Rev. Modern Phys., 62 (1990), pp. 251–342.

[21] M. HELD, P. METZNER, AND F. NOÉ, *Mechanisms of protein-ligand association and its modulation by protein mutations*, Biophys. J., 100 (2011), pp. 701–710.

[22] W. HUISINGA AND B. SCHMIDT, *Metastability and dominant eigenvalues of transfer operators*, in New Algorithms for Macromolecular Simulation, Lect. Notes Comput. Sci. Eng. 49, Springer, Berlin, 2006, pp. 167–182.

[23] R. S. MAIER AND D. L. STEIN, *Limiting exit location distributions in the stochastic exit problem*, SIAM J. Appl. Math., 57 (1997), pp. 752–790.

[24] D. L. MCLEISH AND A. W. KOLKIEWICZ, *Fitting diffusion models in finance*, in Selected Proceedings of the Symposium on Estimating Functions (Athens, GA, 1996), IMS Lecture Notes Monogr. Ser. 32, Institute of Mathematical Statistics, Hayward, CA, 1997, pp. 327–350.

[25] P. METZNER, C. SCHÜTTE, AND E. VANDEN-EIJNDEN, *Illustration of transition path theory on a collection of simple examples*, J. Chem. Phys., 125 (2006), 084110.

[26] F. NOÉ, S. DOOSE, I. DAIDONE, M. LÖLLMANN, J. D. CHODERA, M. SAUER, AND J. C. SMITH, *Dynamical fingerprints for probing individual relaxation processes in biomolecular dynamics with simulations and kinetic experiments*, Proc. Natl. Acad. Sci. USA, 108 (2011), pp. 4822–4827.

[27] F. NOÉ, I. HORENKO, C. SCHÜTTE, AND J. C. SMITH, *Hierarchical analysis of conformational dynamics in biomolecules: Transition networks of metastable states*, J. Chem. Phys., 126 (2007), 155102.

[28] F. NOÉ, C. SCHÜTTE, E. VANDEN-EIJNDEN, L. REICH, AND T. R. WEIKL, *Constructing the full ensemble of folding pathways from short off-equilibrium simulations*, Proc. Natl. Acad. Sci. USA, 106 (2009), pp. 19011–19016.

[29] A. C. PAN AND B. ROUX, *Building Markov state models along pathways to determine free energies and rates of transitions*, J. Chem. Phys., 129 (2008), 064107.

[30] J. D. Pelletier, *A Stochastic Diffusion Model of Climate Change*, preprint, arXiv:ao-sci/9510001, 1995.

[31] M. Rieger, J. Rogal, and K. Reuter, *Effect of surface nanostructure on temperature programmed reaction spectroscopy: First-principles kinetic Monte Carlo simulations of CO oxidation at RuO_2(110)*, Phys. Rev. Lett., 100 (2008), 016105.

[32] W. Ritz, *Über eine neue methode zur lösung gewisser variationsprobleme der mathematischen physik*, J. Reine Angew. Math., 135 (1909), pp. 1–61.

[33] C. C. J. Roothaan, *New developments in molecular orbital theory*, Rev. Modern Phys., 23 (1951), pp. 69–89.

[34] M. Sarich, F. Noé, and C. Schütte, *On the approximation quality of Markov state models*, Multiscale Model. Simul., 8 (2010), pp. 1154–1177.

[35] C. Schütte, A. Fischer, W. Huisinga, and P. Deuflhard, *A direct approach to conformational dynamics based on hybrid Monte Carlo*, J. Comput. Phys., 151 (1999), pp. 146–168.

[36] C. Schütte, F. Noé, J. Lu, M. Sarich, and E. Vanden-Eijnden, *Markov state models based on milestoning*, J. Chem. Phys., 134 (2011), 204105.

[37] C. Schütte, F. Noé, E. Meerbach, P. Metzner, and C. Hartmann, *Conformation dynamics*, in Proceedings of the International Congress on Industrial and Applied Mathematics (ICIAM), R. Jeltsch and G. Wanner, eds., EMS Publishing House, 2009, pp. 297–336.

[38] M. Senne, B. Trendelkamp-Schroer, A. S. J. S. Mey, C. Schütte, and F. Noé, *EMMA: A software package for Markov model building and analysis*, J. Chem. Theory Comput., 8 (2012), pp. 2223–2238.

[39] D. E. Shaw, P. Maragakis, K. Lindorff-Larsen, S. Piana, R. O. Dror, M. P. Eastwood, J. A. Bank, J. M. Jumper, J. K. Salmon, Y. Shan, and W. Wriggers, *Atomic-level characterization of the structural dynamics of proteins*, Science, 330 (2010), pp. 341–346.

[40] N. Singhal and V. S. Pande, *Error analysis and efficient sampling in Markovian state models for molecular dynamics*, J. Chem. Phys., 123 (2005), 204909.

[41] A. Spaar, C. Dammer, R. R. Gabdoulline, R. C. Wade, and V. Helms, *Diffusional encounter of barnase and barstar*, Biophys. J., 90 (2006), pp. 1913–1924.

[42] W. C. Swope, J. W. Pitera, and F. Suits, *Describing protein folding kinetics by molecular dynamics simulations: 1. Theory*, J. Phys. Chem. B, 108 (2004), pp. 6571–6581.

[43] A. Szabo and S. S. Ostlund, *Modern Quantum Chemistry*, Dover, Mineola, NY, 1982.

[44] N. G. van Kampen, *Stochastic Processes in Physics and Chemistry*, 4th ed., Elsevier, Amsterdam, 2006.

[45] V. A. Voelz, G. R. Bowman, K. Beauchamp, and V. S. Pande, *Molecular simulation of ab initio protein folding for a millisecond folder NTL9*, J. Amer. Chem. Soc., 132 (2010), pp. 1526–1528.

[46] S. Meyn W. Huisinga and Ch. Schuette, *Phase transitions and metastability for Markovian and molecular systems*, Ann. Appl. Probab., 14 (2004), p. 419458.

[47] D. J. Wales, *Energy Landscapes*, Cambridge University Press, Cambridge, UK, 2003.

[48] D. J. Wales and J. P. K. Doye, *Stationary points and dynamics in high-dimensional systems*, J. Chem. Phys., 119 (2003), pp. 12409–12416.

[49] M. Weber, *Meshless Methods in Conformation Dynamics*, Ph.D. thesis, 2006.